Chemistry–A European Journal
Research Article
doi.org/10.1002/chem.202401282
Chemistry Europe
European Chemical Societies Publishing
www.chemeurj.org

Can Aromaticity Be Evaluated Using Atomic Partitions Based on the Hilbert-Space?

Joan Grèbol-Tomàs,[a, b] Eduard Matito,*[b, c] and Pedro Salvador*[a]

Dedicated to Miquel Solà on the occasion of his 60th birthday.

Aromaticity is a fundamental concept in chemistry that explains the stability and reactivity of many compounds by identifying atoms within a molecule that form an *aromatic ring*. Reliable aromaticity indices focus on electron delocalization and depend on atomic partitions, which give rise to the concept of an *atom-in-the-molecule* (AIM). Real-space atomic partitions present two important drawbacks: a high computational cost and numerical errors, limiting some aromaticity measures to medium-sized molecules with rings up to 12 atoms. This restriction hinders the study of large conjugated systems like porphyrins and nanorings. On the other hand, traditional Hilbert-space schemes are free of the latter limitations but can be unreliable for the large basis sets required in modern computational chemistry. This paper explores AIMs based on three robust Hilbert-space partitions – meta-Löwdin, Natural Atomic Orbitals (NAO), and Intrinsic Atomic Orbitals (IAO) – which combine the advantages of real-space partitions without their disadvantages. These partitions can effectively replace real-space AIMs for evaluating the aromatic character. For the first time, we report multicenter index (MCI) and I_{ring} values for large rings and introduce ESIpy, an open-source Python code for aromaticity analysis in large conjugated rings.

1. Introduction

Although aromaticity is an ill-defined chemical concept, it is one of the most widely used to rationalize the stability and reactivity of many chemical compounds.[1–3] Since aromaticity is not a directly measurable quantity, several definitions of aromaticity have been put forward.[4–8] With the discovery of new aromatic compounds,[8] some of these definitions have become obsolete and new quantities rooted on quantum mechanics have been proposed. Most of these measures rely one way or another on the identification of atoms in the molecule, as these atoms constitute the *aromatic ring* which is the subject of study. This is particularly relevant for the measures of aromaticity based on electron delocalization,[5,9,10] which hinge on the definition of an *atom-in-the-molecule* (AIM). Among them, the multicenter delocalization indices[11–16] have been shown to perform particularly very well as all-around aromaticity indicators.[17,18] Multicenter indices originate from generalized atomic population analysis[13] so a proper identification of the AIM is essential.

There are two main ways to define the AIM, either partitioning the Hilbert-space or the physical space. The former relies on the widespread use of atom-centered basis functions to expand the molecular orbitals (*i.e.*, on the LCAO-MO approximation[19]). Each atom is identified by its nucleus and the set of basis functions or atomic orbitals (AO) associated with it.[20] In real-space methods, on the contrary, the atom is identified by its nucleus and a region of the physical space (atomic basin).[21–23]

Real-space methods such as the Quantum Theory of Atoms in Molecules (QTAIM),[24] are often preferred because of their insensibility with the AO basis set used to compute the molecular wavefunction.[25,26] The main ingredient of MCI is the atomic overlap matrices (AOM) $\mathbf{S}^A$, with elements

$$S_{ij}^A = \int_{\Omega_A} \phi_i^*(\mathbf{r})\phi_j(\mathbf{r})\mathrm{d}\mathbf{r}\,, \tag{1}$$

where the integration is carried out (numerically) on the atomic basin. While QTAIM is one of the most widely used AIM partitioning, offering realible results that other partitions fail to give,[22,27–29] it has some drawbacks. One of the primary limitations lies in the complexity and rather high computational cost of the numerical integration of density functions over the atomic domains.[30] Furthermore, the challenge of obtaining sufficiently precise numerical integrations can lead to numerical errors when calculating electronic structure indicators derived from Eq. 1.[31]

In Hilbert-space schemes, the standard practice involves operating within the AO basis representation and collecting

[a] Mr. J. Grèbol-Tomàs, Dr. P. Salvador
Departament de Química, Universitat de Girona
Campus de Montilivi, 17071 Girona (Spain)
E-mail: pedro.salvador@udg.edu
[b] Mr. J. Grèbol-Tomàs, Dr. E. Matito
Donostia International Physics Center (DIPC), Manuel de Lardizábal 4, 20018 Donostia, Euskadi (Spain)
E-mail: ematito@dipc.org
[c] Dr. E. Matito
Ikerbasque Foundation for Science, Bilbao, Euskadi (Spain)

Supporting information for this article is available on the WWW under https://doi.org/10.1002/chem.202401282

different contributions according to the indices of the AO basis. This is how well-established quantities such as Mulliken's population analysis[20] or Mayer's bond orders are articulated.[32] Alternatively, one can readily see that the following AOM

$$\mathbf{S}^{\mathrm{A,Mull}} = \mathbf{c}^{+}\mathbf{S}^{\mathrm{AO}}\boldsymbol{\eta}^{\mathrm{A}}\mathbf{c}, \tag{2}$$

where $\mathbf{c}$ collects the coefficients of the occupied MOs, $\mathbf{S}^{\mathrm{AO}}$ is the overlap matrix of the original AO basis, and $\boldsymbol{\eta}^{\mathrm{A}}$ is a block-truncated unit matrix with all elements being zero except $\eta^{\mathrm{A}}_{\mu\mu} = 1$ for $\mu \in \mathrm{A}$, can be used instead of Eq. 1 in the MO representation formulae.

However, relying solely on the original AO basis of the electronic structure computation presents several limitations. Firstly, the outcome of the analysis heavily hinges on the chosen one-electron basis.[33] Although minimal basis sets suffice for achieving a qualitative grasp of the molecular wave function, they often fall short for quantitative molecular properties or thermodynamics. Conversely, large basis sets, particularly those incorporating diffuse functions, lack atomic character and are not suitable for direct Hilbert-space analysis.[31,33] One way to sort out these problems is to carry out an orthogonalization of the original AO basis, and then perform the Hilbert-space analysis on the new orthogonal basis. In this case, the mapping for the AOM can be generally expressed as

$$\mathbf{S}^{\mathrm{A,T}} = \mathbf{c}^{+}(\mathbf{T}^{-1})^{+}\boldsymbol{\eta}^{\mathrm{A}}\mathbf{T}^{-1}\,\mathbf{c}, \tag{3}$$

where $\mathbf{T}$ is the transformation matrix from the original AO basis to the orthonormalized one. The simplest form is $\mathbf{T} = (\mathbf{S}^{\mathrm{AO}})^{1/2}$, corresponding to Löwdin's symmetric orthogonalization.[34]

In the meta-Löwdin scheme (m-Löwdin),[35] occupancy-averaged atomic Hartree-Fock calculations are used as a reference to project out the core orbitals. Then, Löwdin orthogonalization is carried out separately for the core and the valence spaces.

The occupancy-weighted symmetric orthogonalization is a generalization of Löwdin's scheme

$$\mathbf{T} = \left(\mathbf{W}^{+}\mathbf{S}^{\mathrm{AO}}\mathbf{W}\right)^{1/2}\mathbf{W}, \tag{4}$$

where an additional weight matrix, $\mathbf{W}$, is introduced. In the natural atomic orbitals (NAO) procedure,[36] the symmetrized atomic blocks of the density are diagonalized to obtain the occupations of the valence space, which are then used to build $\mathbf{W}$.

The Intrinsic Atomic Orbitals (IAO) from Knizia have also gained recent interest.[37] The IAO procedure relies on a reference minimal basis set, with rank predetermined by the free atom electron configuration. The procedure involves several projections to the reference minimal basis and back to the original one to generate a new orthogonal minimal basis (the IAO basis) which *exactly* expands the occupied MOs (and thus the density). Hence, the resulting transformation matrix $\mathbf{T}$ is rectangular.

IAOs and particularly NAOs have been extensively used for population analysis,[38–42] proving their basis set independence. Together with the newly developed meta-Löwdin scheme, represent three promising alternatives to classical Mulliken or Löwdin partitionings to account for electron delocalization in molecular systems.

One of the first links between cyclic electron delocalization and aromaticity was Giambiagi's[11] I_{ring} multicenter index,[14] defined for restricted single-determinant wavefunctions as

$$I_{\mathrm{ring}}\,(A) = 2^{n}\sum_{i_1,i_2,\ldots,i_n} \mathrm{S}^{\mathrm{A}_1}_{i_1 i_2}\mathrm{S}^{\mathrm{A}_2}_{i_2 i_3}\cdots\mathrm{S}^{\mathrm{A}_n}_{i_n i_1}, \tag{5}$$

where A represents a set of n connected atoms $\{\mathrm{A}_1,\mathrm{A}_2,\cdots,\mathrm{A}_n\}$ forming a ring. Bultinck and coworkers[15] suggested the Multicenter Index (MCI) considering the I_{ring} values for all $n!$ permutations of the positions of the atoms in A, generated by $P(A)$,

$$\mathrm{MCI}(A) = \frac{1}{2n}\sum_{P(A)} I_{\mathrm{ring}}(A) \tag{6}$$

Unlike I_{ring} , MCI is by definition invariant to the position of the atoms in the string A, hence, it can be used to measure electron delocalization in an array of atoms, even if they do not define a closed circuit. Unfortunately, the complexity of MCI grows exponentially with the size of the ring (n), which makes it only applicable to a small array of atoms. Both I_{ring} and MCI have been used in the literature to quantify cyclic delocalization, usually in combination with real-space AIMs such as QTAIM.[5,16,43] It has been shown that Hilbert-space methods like Mulliken's but also using Löwdin's orthogonalized basis yield unreliable, basis set dependent, numerical values of the indices.[31] On the other hand, the accuracy of the numerical integrations over the atomic basins using QTAIM or other approaches can largely affect both I_{ring} and (especially) MCI values for large rings, because of error accumulation. Eventually, their values tend to become increasingly inaccurate and smaller. This limitation poses a challenge when applying robust real-space methods to analyze the aromaticity in larger systems.[31]

To address these challenges, one of us proposed the AV1245 index,[31] aimed at performing a similar task to MCI but without exhibiting exponential scaling with the system size or accumulating significant error with increasing ring length. AV1245 averages all the four-center MCI values along the ring while maintaining the positional relationship of 1,2,4,5, thus leading to

$$\mathrm{AV1245}(A) = \frac{1000}{3}\sum_{i=1}^{n}\mathrm{MCI}(\mathrm{A}_i,\mathrm{A}_{i+1},\mathrm{A}_{i+3},\mathrm{A}_{i+4}), \tag{7}$$

where if $i > n$ A_i should be replaced by A_{i-n}. In addition, we also defined the $\mathrm{AV}_{\mathrm{min}}$ index as the minimum (absolute) value of all the four-center MCI indices that enter the AV1245 expression. AV1245 and $\mathrm{AV}_{\mathrm{min}}$ capture multicenter delocalization while avoiding computing indices involving all n centers of the ring, thus minimizing the lack of precision, drastically reducing the computational cost, and size-extensivity problems. A high AV1245 or $\mathrm{AV}_{\mathrm{min}}$ value is related to the aromatic character of

the ring and these indices cannot be computed for less than six-member rings (6-MR). AV_{min} has been shown to reproduce the annulene pathway as the most conjugated pathway in neutral (extended) porphyrins.[44] Other aromaticity indices based on QTAIM partitions have also been put forward.[45–50]

In contrast to real-space methods, Hilbert-space schemes offer an exact (analytical) form of the AOM. Consequently, the computation of multicenter indices within the Hilbert-space framework is naturally devoid of numerical errors, ensuring a high level of accuracy even for larger-sized rings. The goal of this work is twofold. On one hand, we will explore the use of robust Hilbert-space schemes for the calculation of aromaticity indicators, namely I_{ring}, MCI, and AV1245, assessing their basis set dependency and comparing the behavior to previous QTAIM-based results. We will study some selected examples that thus far could not be computed. On the other hand, we present the official release note of ESIpy. This open-source code is hosted and maintained on Github[1] where the release notes and documentation can also be found. The idea is stablishing IAO, NAO, and meta-Löwdin atomic partitions as an economical and realiable way to compute aromaticity, and extend the applicability of these methods to systems that thus far could not be addressed using electronic aromaticity measures based on real-space atomic partitions.

2. Computational Details

In this work, we will consider three sets of molecules. The first set includes mostly polycyclic aromatic hydrocarbons (PAHs) optimized at the B3LYP/aug-cc-pVDZ level: cyclohexane, pyridine, benzene, naphthalene, anthracene, phenanthrene, tetracene, and pyridine. Some molecules of this set will be employed to analyze the basis set dependence of the aromaticity indicators using various atomic partitions, whereas part of this set will be used to assess the performance of electronic aromaticity measures based on Hilbert-space analyses. The second molecular set involves cyclobutadiene, benzene, cyclooctatriene, [10]annulene, [12]annulene, [14]annulene, two conformations of [16]annulene, [18]annulene. The Cartesian coordinates of annulenes have been obtained at the B3LYP/6-311G** level of theory. The third set includes E_{12}^{2-} spherenes (E = Ge, Sn, Pb) and their geometries were optimized at the SO-ZORA-BP86/TZ2P level of theory in Ref. [51]. For spherenes, single-point calculations have been performed at the B3LYP/def2-tZVP level. In all cases, we have used Gaussian's definition of B3LYP, which uses VWN80.[52]

Since B3LYP is a DFA prone to present delocalization errors,[44,53–57] in Section S6 of the Supporting Information we have provided all the data of this manuscript at the CAM–B3LYP level of theory.

The in-house program, ESIpy, has been developed using Python and PySCF's[39,58,59] tools and encompasses a collection of functions for computing aromaticity indices (FLU,[45,46] PDI,[48] BOA,[55] Iring,[14] MCI[15]) from a Hilbert-space partition. The real-space counterparts have been obtained using ESI-3D[22,45,60] and AIMAll.[61] Single-point calculations and optimizations have been performed with PySCF and Gaussian.[62]

[1] https://github.com/jgrebol/ESIpy

3. Basis Set Dependency

Unlike real-space partitions, Hilbert-space partitions can be highly basis-set dependent.[25,31,33,63] The latter limits the applicability of electronic structure indicators based on such partitions, which thus far could not be employed in electronic aromaticity descriptors.[31] In this first section, we will test the basis dependence of two of the most reliable electronic aromaticity indices,[17,18] MCI and I_{ring}, in a set of polycyclic aromatic hydrocarbons (PAHs) using five Hilbert-space partitions (Mulliken, Löwdin, meta-Löwdin, NAO, and IAO). The results are gathered in Table 1 for benzene, including values for thirteen different basis sets. Results obtained for other PAH align with those obtained for benzene and are included in Tables S1—S6 of the Supporting Information. Other electronic aromaticity indicators, such as BOA, FLU, and PDI are also included in Tables S7—S13 for completeness.

From the results in Table 1 is evident that the use of Mulliken's or Löwdin partitions, as expected, yields highly inconsistent results, as the values obtained using different basis sets do not exhibit any discernible pattern. Conversely, both meta-Löwdin and IAO approaches showcase very high consistency regardless of the basis set employed, being both good options for the calculation of aromaticity indices. On the other hand, NAO exhibits a relatively high level of consistency, albeit not as robust as meta-Löwdin or IAO.

In Table 1, we notice that for some large basis sets, such as aug-cc-pVDZ and aug-cc-pVQZ, the values of I_{ring} and MCI obtained for Mulliken and Löwdin partitions deviate most significantly. The latter finding prompted us to explore the effect of near-linear dependencies of the AO basis. When solving the SCF equations, the generalized eigenvalue problem is typically transformed into a conventional eigenvalue problem with the $(\mathbf{S}^{AO})^{1/2}$ matrix. A threshold for the eigenvalues of **S**AO is introduced so that the eigenvectors with eigenvalues below the threshold are discarded in the canonic orthogonalization procedure. As a result, some (linear combination of) basis functions are removed from the calculation. Table 2 gathers the MCI values obtained for naphthalene and anthracene at the B3LYP/aug-cc-pVDZ level for different values of the near-linear dependency threshold. A similar table for the I_{ring} values can be found in the SI (see Table S14). It can be seen that the effect of removing basis functions in the SCF procedure has an enormous impact on Mulliken's MCI values, while for the other schemes, the results are essentially unaltered. Using the default threshold in some programs[62] (10^{-6}) is clearly insufficient to correct the disparate MCI values. Increasing the threshold beyond this value removes more basis functions and Mulliken's MCI values decrease, but not in a monotonic way. With a threshold as large as 10^{-4} the MCI values seem rather converged, yielding values in line with those obtained with NAO basis. Conversely, Löwdin's values are insensitive to the

Table 1. MCI and I_{ring} values for benzene using different Hilbert-space schemes and basis sets.

		Mulliken	Löwdin	m-Löwdin	NAO	IAO
I_{ring}	STO-3G	0.088	0.088	0.088	0.088	0.088
	6-31G**	0.085	0.072	0.087	0.087	0.088
	6-31+G**	0.087	0.072	0.087	0.086	0.088
	6-31++G**	0.092	0.072	0.087	0.086	0.088
	6-311G**	0.078	0.062	0.087	0.087	0.088
	6-311+G**	0.080	0.062	0.087	0.087	0.088
	6-311++G**	0.096	0.062	0.087	0.087	0.088
	cc-pVDZ	0.077	0.053	0.087	0.087	0.088
	cc-pVTZ	0.065	0.019	0.087	0.087	0.088
	cc-pVQZ	0.063	0.005	0.087	0.085	0.088
	aug-cc-pVDZ	0.461	0.004	0.086	0.083	0.088
	aug-cc-pVTZ	0.065	0.000	0.086	0.083	0.088
	aug-cc-pVQZ	0.121	−0.001	0.086	0.082	0.088
MCI	STO-3G	0.132	0.132	0.132	0.132	0.132
	6-31G**	0.127	0.107	0.131	0.131	0.132
	6-31+G**	0.138	0.108	0.130	0.129	0.132
	6-31++G**	0.148	0.107	0.130	0.129	0.132
	6-311G**	0.118	0.093	0.130	0.130	0.132
	6-311+G**	0.125	0.093	0.130	0.130	0.132
	6-311++G**	0.188	0.093	0.130	0.130	0.132
	cc-pVDZ	0.115	0.080	0.130	0.130	0.132
	cc-pVTZ	0.099	0.036	0.130	0.130	0.132
	cc-pVQZ	0.102	0.021	0.129	0.128	0.132
	aug-cc-pVDZ	0.745	0.020	0.129	0.124	0.132
	aug-cc-pVTZ	0.105	0.015	0.129	0.124	0.132
	aug-cc-pVQZ	0.257	0.021	0.128	0.123	0.132

Table 2. MCI values obtained at the B3LYP/aug-cc-pVDZ level using different values for the near-linear dependency threshold. Nbas is the actual number of basis functions used in the SCF procedure.

	Threshold	Nbas	Mulliken	Löwdin	m-Löwdin	NAO	IAO
Benzene	None	192	0.745	0.020	0.129	0.124	0.132
	4.00E-06	190	0.304	0.020	0.129	0.124	0.132
	8.50E-06	189	0.304	0.020	0.129	0.124	0.132
	2.10E-05	187	0.119	0.020	0.129	0.124	0.132
	3.20E-05	186	0.119	0.020	0.129	0.124	0.132
	4.80E-05	184	0.079	0.020	0.129	0.124	0.132
	1.10E-04	179	0.112	0.020	0.129	0.124	0.132
Naphthalene	None	302	6.473	0.010	0.070	0.066	0.071
	1.00E-06	301	5.694	0.010	0.070	0.066	0.071
	1.40E-06	300	5.635	0.010	0.070	0.066	0.071
	5.00E-06	296	0.400	0.010	0.070	0.066	0.071
	1.00E-05	294	0.958	0.010	0.070	0.066	0.071
	5.00E-05	284	0.065	0.010	0.070	0.066	0.071
	1.00E-04	278	0.060	0.010	0.070	0.066	0.071

threshold, but the values are clearly underestimated, especially for I_{ring} (see Table S14). Thus, while near-linear dependencies seem to be a major factor in the pathological MCI and I_{ring} values obtained with the Mulliken partition, the required threshold is way too large to be used in practical applications.

4. QTAIM Versus Hilbert-Space Methods

Thus far, we have established meta-Löwdin, IAO, and NAO as robust Hilbert-space atomic partitions, demonstrating minimal basis set dependence. In this section, we investigate the potential of these partitions to serve as reliable alternatives for computing aromaticity indices. In Table 3, normalized I_{ring} and MCI, *i.e.* $I_{ring}^{1/n}$ ring and MCI$^{1/n}$, and AV1245 are compared for several 6MRs using both QTAIM and robust Hilbert-space partitions. For the values of PDI, BOA, and FLU indices using the latter partitions, see Table S15 of the Supporting Information.

In Figure 1, we present the correlations between these three Hilbert-space schemes and QTAIM for I_{ring}, MCI, and AV1245. All correlations between robust Hilbert-space schemes and QTAIM are excellent. The numerical values of the indices using Hilbert-space partitions are systematically larger compared to QTAIM. In Figure S1, we give the bonded C–C delocalization indices (DI)[22,64] for the PAH listed in Table 3 (the DI are the two-atom analogs of MCI). The correlation is very similar to that found for MCI and I_{ring}, as in all cases we have normalized the quantities per atom, *i.e.*, we analyzed the values of MCI$^{1/n}$, $I_{ring}^{1/n}$, and DI$^{1/2}$. Since AV2145 is based on the *average* four-atom MCI values, we cannot effectively normalize AV1245 per atom, and hence, the

Table 3. $I_{ring}^{1/n}$, $MCI^{1/n}$ and AV1245 for various six-membered rings in a series of PAHs using Hilbert-space partitions and QTAIM at the B3LYP/aug-cc-pVDZ level of theory. $I_{ring}^{1/n}$ ring values are computed as $\text{sign}(I_{ring})\,|I_{ring}|^{1/n}$, and $MCI^{1/n}$ similarly.

		m-Löwdin	NAO	IAO	QTAIM
$I_{ring}^{1/n}$	**Cyclohexane**	0.282	0.266	0.282	0.258
	Benzene	0.665	0.660	0.667	0.604
	Naphthalene	0.606	0.600	0.608	0.551
	Anthracene (out)	0.582	0.576	0.584	0.529
	Anthracene (in)	0.572	0.566	0.575	0.520
	Phenanthrene (out)	0.623	0.617	0.625	0.565
	Phenanthrene (in)	0.541	0.534	0.525	0.492
$MCI^{1/n}$	**Cyclohexane**	0.279	0.267	0.280	0.264
	Benzene	0.711	0.706	0.714	0.643
	Naphthalene	0.641	0.636	0.644	0.580
	Anthracene (out)	0.612	0.606	0.614	0.553
	Anthracene (in)	0.603	0.596	0.605	0.545
	Phenanthrene (out)	0.661	0.656	0.664	0.598
	Phenanthrene (in)	0.564	0.557	0.566	0.510

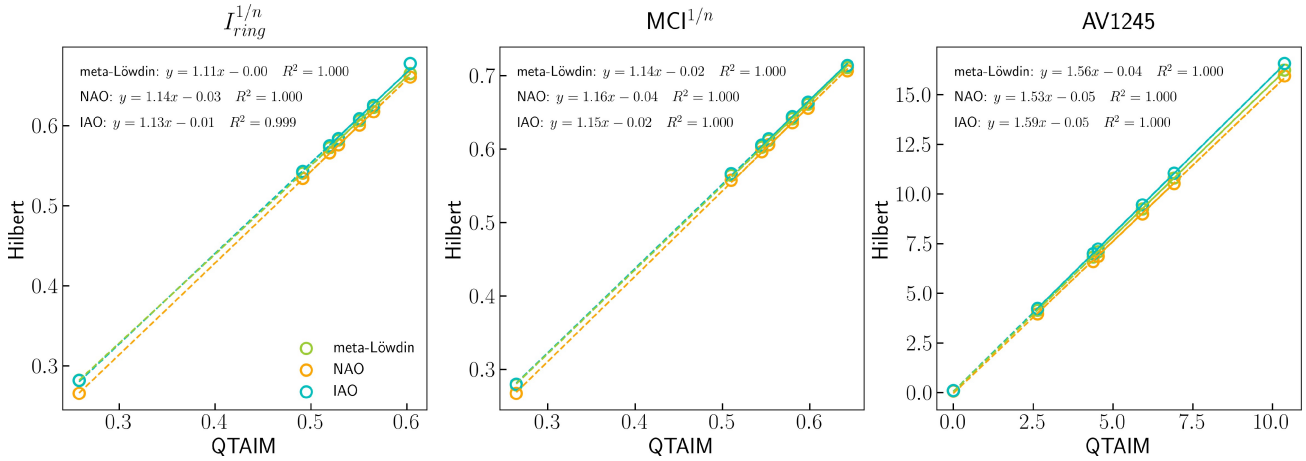

Figure 1. $I_{ring}^{1/n}$ $MCI^{1/n}$ and AV1245 from robust Hilbert-space schemes (meta-Löwdin, NAO, and IAO) against QTAIM for the PAHs of Table 3.

larger AV2145 values displayed in Figure 1 are about 50% higher with Hilbert-space partitions, as opposed to the ca. 10% increased observed for normalized quantities. The increase of aromaticity indices using Hilbert-space schemes does not affect the general trends of these quantities, confirming these partitions can effectively replace QTAIM in routine analyses.

These robust Hilbert-space partitions also maintain some basic precepts of aromaticity measures. For instance, according to all the indices and all atomic partitions, cyclohexane exhibits the lowest aromatic character and benzene is the most aromatic species in the series, a prescription which is violated by other atomic partitions.[28] We also confirm that the relative aromaticity of annealed rings in PAH is maintained for these Hilbert-space schemes. Following Clar's sextet rules,[65] the outer rings of phenanthrene are more aromatic than the inner ones because the resonant structure with the largest number of aromatic π-sextets, the Clar structure, corresponds to two π-sextets in the external six-member rings of phenanthrene.[45,66] Conversely, for anthracene, all resonant structures have only one π-sextet, which *migrates* among the three six-member rings.[65] For this reason, there is only a small difference in the aromaticity of the outer and inner rings of anthracene, as confirmed by all the aromaticity descriptors regardless the atomic partition employed.[45,66] Interestingly, these Hilbert space partitions also identify the *para*-DI of benzene as larger than the *meta*-DI (see Table S18), which is a basic condition for the para-delocalization index (PDI).[48,67]

In Table S16, we collect values for Mulliken and Löwdin partitions of the same molecules and indices gathered in Table 3. We observe that many of the previous precepts are violated. For instance, benzene is never the most aromatic species as measured from MCI and I_{ring} using Mulliken's partition. In addition, according to Mulliken's MCI values, phenanthrene's inner six-member ring is found more aromatic than the outer one and there is a sensible difference between the inner and the outer rings of anthracene. Löwdin's values of I_{ring} are too small for both anthracene and phenanthrene. All these flaws are entirely due to the unreliability of Mulliken and Löwdin's atomic partitions. Conversely, AV1245 seems to be less sensitive to the atomic partition, giving qualitatively reasonable values for this series of PAH at the B3LYP/aug-cc-pVDZ level of theory using Löwdin's partition.

5. Aromaticity Indicators on Annulenes

In the previous sections, we have showed the reliability of IAO, NAO, and meta-Löwdin atomic partitions to compute aromaticity measures. However, all the species studied thus far could be easily computed using a real-space partition, such as QTAIM. As the size of the aromatic ring increases, some indices like I_{ring} and MCI accumulate important numerical integration errors, which cast a shadow of doubt on the values we can obtain.[31] In this section, we study a series of annulenes, and demonstrate that robust Hilbert-space analyses, which are exempt of numerical errors, can be employed to compute MCI and I_{ring} values of large aromatic rings. Since MCI's cost grows exponentially with the ring size regardless of the atomic partition, we will explore only I_{ring}. Reducing the computational cost of MCI will be the subject of a forthcoming work. For the sake of completeness, we will also study the performance of AV1245[31] and AV_{min}[68] indices, which were intentionally designed for large rings. Following the Hückel's rule, annulenes are separated into antiaromatic and aromatic ones and collected in Table 4.

Once more, there is a good agreement between quantities computed from robust Hibert-space partitions and the corresponding QTAIM values obtained from Ref. [55], the only exception being cyclobutadiene. Indeed, as we can see in Figure 2, all annulenes follow the linear correlation taken from PAHs (Figure 1) except for cyclobutadiene. A careful analysis of the latter system reveals that the discrepancies between atomic

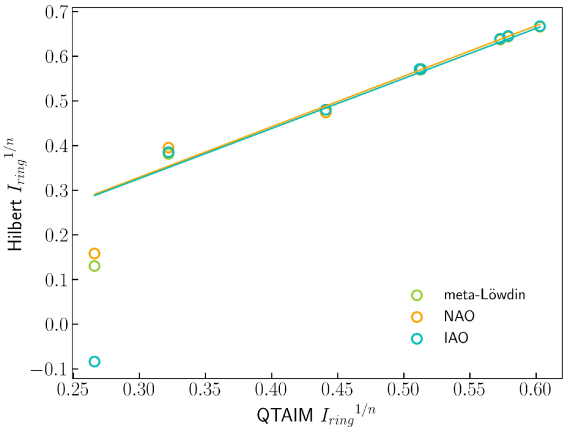

Figure 2. IAO, NAO, and meta-Löwdin $I_{ring}^{1/n}$ values against QTAIM for the annulenes of Table 4. The linear plots correspond to the linear regression equations obtained for PAH in Figure 1.

partitions are not limited to I_{ring} values. The DIs between two single (double) C–C bonds are 0.97 (2.01), 0.97 (2.00), 0.98 (2.00), and 0.97 (1.87), for IAO, NAO, meta-Löwdin, and QTAIM, respectively (see Table S17 for all DIs of cyclobutadiene). Hence, while C–C bonds are fairly similar among different partitions, C=C ones are clearly more localized in Hilbert-space partitions, contributing to a less aromatic four-member ring. In this sense, the values of I_{ring} are consistent with the DIs. Among all the

Table 4. $I_{ring}^{1/n}$ and AV1245 for the various annulenes computed at the B3LYP/6-311G** level of theory. $I_{ring}^{1/n}$ values are computed as $\mathrm{sign}(I_{ring})\,|I_{ring}|^{1/n}$. [a] The I_{ring} values for these rings were too small for an accurate calculation of the $I_{ring}^{1/n}$. [b] Values from Ref. [55].

		4n + 2 species			
		m-Löwdin	NAO	IAO	QTAIM[b]
$I_{ring}^{1/n}$	**Benzene**	0.666	0.666	0.667	0.603
	[10]annulene(twist)	0.381	0.395	0.385	0.322
	[10]annulene(heart)	0.644	0.644	0.645	0.579
	[14]annulene	0.635	0.635	0.636	–[a]
	[18]annulene	0.637	0.638	0.639	0.573
AV1245	**Benzene**	16.385	16.378	16.567	10.721
	[10]annulene(twist)	0.269	0.302	0.253	0.216
	[10]annulene(heart)	8.123	8.173	8.256	5.416
	[14]annulene	6.701	6.774	6.820	4.436
	[18]annulene	6.481	6.545	6.601	4.372
		4n species			
$I_{ring}^{1/n}$	**Cyclobutadiene**	0.130	0.158	−0.084	0.266
	Cyclooctatriene	0.480	0.474	0.480	0.441
	[12]annulene	0.497	0.500	0.499	–[a]
	[16]annulene(S4)	0.570	0.570	0.571	0.512
	[16]annulene(C1)	0.570	0.570	0.571	0.513
AV1245	**Cyclooctatriene**	−1.178	−1.099	−1.240	−0.721
	[12]annulene	0.809	0.855	0.804	0.582
	[16]annulene(C1)	1.674	1.738	1.689	1.173
	[16]annulene(S4)	1.641	1.699	1.653	1.156

systems studied in this work, cyclobutadiene is the only one presenting quantitative differences among robust Hilbert-space partitions and QTAIM. Fortunately, small rings are not a limitation of real-space partitions. Interestingly, with these robust Hilbert-space partitions, we can provide a $I_{ring}^{1/n}$ value for [12]annulene, which could not be obtained from a QTAIM partition because the I_{ring} value was too small to provide a reliable $I_{ring}^{1/n}$ value. [12]annulene, is thus confirmed as an antiaromatic species with values very close to cyclooctatriene.

In Figure 3 and Figure S3, we confirm that robust Hilbert-space partitions are a perfect replacement for the QTAIM partition for computing AV1245 and AV_{min}. In fact, the latter index has been shown to exhibit a more robust account of aromaticity in extended systems,[44,69] in agreement with the excellent correlation between $I_{ring}^{1/n}$ and AV_{min} (see Figure S4).

6. 3D-Aromaticity on Spherenes

In this section, we study the three-dimensional aromaticity of E_{12}^{2-} (E = Ge, Sn, Pb) spherenes. The latter two icosahedral inorganic fullerene analogues were synthesized in 2006[70,71] and their aromaticity was characterized using magnetic responses properties (NICS and $\mathbf{B}_{ind}$).[51,72] It is well known that response aromaticity, as measured from the magnetic response of the system, sometimes gives a conflicting conclusion with the intrinsic aromatic character of the system, measured from electron delocalization.[56,57,73–79]

Since the aromaticity in these spherenes is due to delocalization over the *surface* of the spherene, indices that require a close loop, such as FLU, AV1245, or I_{ring} cannot be employed. Conversely, MCI considers the delocalization among a collection of atoms, regardless they form a ring structure or not. Hence, MCI is the only electronic aromaticity criterion that can be straightforwardly applied to assess the delocalization among an array of atoms forming a surface or a volume. Thus far, these systems could not be studied using MCI because real-space calculations carry a large numerical error, as we have seen in the previous section. Nevertheless, since we can compare real-space calculations with robust Hilbert-space partitions, in this work, we will also include QTAIM values for the sake of comparison.

We took the geometries optimized at the SO-ZORA-BP86/TZ2P from Ref. [51], which include relativistic effects and performed single-point calculations at the B3LYP/def2-tZVP level of theory, the results of which are collected in Table 5. Magnetic quantities are affected by relativistic effects,[51,80] while electron delocalization measures – being mostly driven by valence electrons – are barely affected as long as the geometries are optimized including relativistic corrections.[81,82] Castro et al.[51] realized the inclusion of relativistic effects changed the magnetic description of stannaspherene from antiaromatic to aromatic, whereas in plumbaspherene the relativistic effects were necessary to identify the molecule as aromatic instead of nonaromatic. Interestingly, the $MCI^{1/n}$ values of the three systems are qualitatively similar among them, suggesting they have a similar aromatic character – as concluded from magnetic responses studies. Their $MCI^{1/n}$ values are lower than those of benzene, yet comparable to other less aromatic systems, such as anthracene. Therefore, this spherene family can be considered 3D-aromatic from all points of view.

7. Local Versus Global Aromaticity

In Section 4, we analyzed the local aromaticity of the six-member rings of anthracene and phenanthrene and found that aromaticity measures aligned well with the expected Clar structures in these molecules. However, we ignored the delocalization along larger rings, such as those formed by the carbon perimeter of these molecules (14 atoms) and the ring formed by two annealed rings (10 atoms). A ring current analysis reveals that the preferred delocalization pathways in these molecules occur along their carbon perimeters.[83] The magnetic rings current is a *response aromatic* property and electron delocalization, as measured from I_{ring} and the other indices presented in this paper is an *intrinsic aromatic* property. Hence, they are not expected to agree with each other. However, some authors have reconciled these properties for particular cases, being the study of PAH one of them.[84] The latter study employed the pseudo-π model, which greatly simplifies the calculation of MCI but it can only be employed in planar molecules. Robust Hilbert-space schemes are not limited to planar systems and, with our current implementation, we can routinely compute MCI values for $n \leq 14$. In Table 6, we collect the $MCI^{1/n}$ values of all the rings in anthracene and phenanthrene. The results confirm that the perimeter ($n = 14$) is

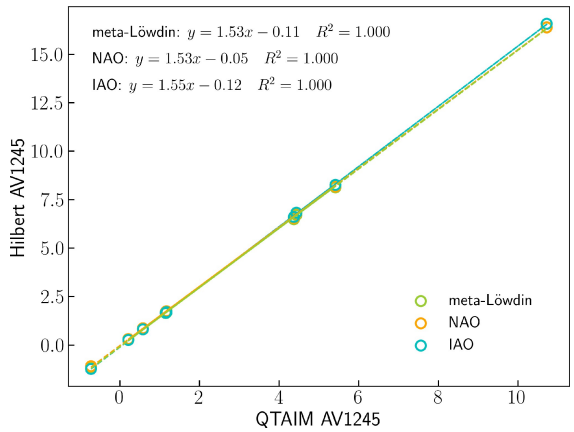

Figure 3. AV1245 linear regression versus QTAIM using IAO, NAO, and meta-Löwdin for the selected molecules.

Table 5. $MCI^{1/n}$ values for the set of spherenes E_{12}^{2-} (E = Ge, Sn, Pb). [b] QTAIM values are prone to significant numerical errors, and thus, these values should be considered only as qualitative indicators.

	m-Löwdin	NAO	IAO	[b]QTAIM
Ge	0.608	0.606	0.612	0.538
Sn	0.581	0.576	0.568	0.538
Pb	0.610	0.586	0.577	0.534

Table 6. $MCI^{1/n}$ values for the different 6-, 10- and 14-member rings of anthracene and phenanthrene computed at the B3LYP/aug-cc-pVDZ level of theory.

		m-Löwdin	NAO	IAO	QTAIM
Benzene	$n=6$	0.711	0.706	0.714	0.643
Anthracene	$n=6$ (outer)	0.612	0.606	0.614	0.553
	$n=6$ (inner)	0.603	0.596	0.605	0.545
	$n=10$	0.666	0.661	0.669	0.602
	$n=14$	0.695	0.690	0.698	0.629
Phenanthrene	$n=6$ (outer)	0.661	0.656	0.664	0.598
	$n=6$ (inner)	0.564	0.557	0.566	0.510
	$n=10$	0.645	0.639	0.648	0.584
	$n=14$	0.690	0.685	0.693	0.625

the preferred conjugation pathway, with values not far from those reported for benzene. Therefore, it could be argued that the global aromaticity of these PAHs is similar to that of benzene, while their local aromaticity within six-membered rings is distinctly lower than the latter.

8. Conclusions

In this paper, we have demonstrated that robust Hilbert-space atomic partitions, including IAO, NAO, and meta-Löwdin, present a promising alternative for replacing real-space partitions in calculating electron delocalization and aromaticity measures. These partitions not only offer a computationally more economical approach but also eliminate numerical integration errors. The limitations imposed by these errors and computational demands significantly restricted the size of the molecules and, crucially, the size of the conjugated rings that could be analyzed thus far. Through the study of various aromatic molecules of differing natures and sizes, we have shown that these partitions can be effectively used to assess aromaticity.

We have also demonstrated the robustness of the IAO, NAO, and meta-Löwdin partitions with respect to the size of the basis set, a characteristic they share with real-space analysis but which contrasts with traditional Hilbert-space partitions such as Mulliken or Löwdin. While the accuracy of Mulliken partitioning can be enhanced by carefully removing linear dependencies in the basis set, its application is not advisable. This is because achieving sensible results necessitates significantly compromising the quality of the basis, undermining the reliability of the outcomes.

Finally, we have achieved the first non-approximate MCI calculations for large rings or surfaces for up to n = 14, including anthracene, phenanthrene, and three spherenes, as well as even larger structures like [18]annulene, utilizing I_{ring}. These results set the stage for future work, as outlined in a forthcoming paper, where we will introduce an approximate scheme designed to overcome the exponential computational barrier associated with MCI calculations. This approach promises to extend our capability to analyze even larger molecular structures.

We have also introduced ESIpy, a Python code now available for conducting calculations that were previously prohibitive. This tool will significantly aid in advancing our understanding of the aromaticity of large conjugated structures.

Acknowledgements

The authors acknowledge funding from Agencia Española de Investigación, "FEDER Una manera de hacer Europa" (PID2022-140666NB-C21 and PID2022-140666NB-C22), the Donostia International Physics Center (DIPC-INV-003132, DIPC-INV-003133), the Generalitat de Catalunya (2021 SGR00623), and the grants funded by the Gobierno Vasco (IT1584-22, and PIBA_2023_1_0055). Calculations were performed on the computing facilities provided by the DIPC. Technical and human support provided by IZO-SGI, SGIker (UPV/EHU, MICINN, GV/EJ, ERDF, and ESF), and MCIA is gratefully acknowledged.

Conflict of Interests

The authors declare no conflict of interest.

Data Availability Statement

The data that support the findings of this study are available in the supplementary material of this article.

Keywords: Aromaticity · Electron delocalization · Computational Chemistry · Extended Systems · Atomic Partition

[1] M. Solà, *Front. Chem.* **2017**, *5*, 22.
[2] P. von Ragué Schleyer, H. Jiao, *Pure Appl. Chem.* **1996**, *68*, 209.
[3] G. Frenking, A. Krapp, *J. Comput. Chem.* **2007**, *28*, 15.
[4] J. Poater, M. Duran, M. Solà, B. Silvi, *Chem. Rev.* **2005**, *105*, 3911.
[5] F. Feixas, E. Matito, J. Poater, M. Solà, *Chem. Soc. Rev.* **2015**, *44*, 6389.
[6] Z. Chen, C. S. Wannere, C. Corminboeuf, R. Puchta, P. v R Schleyer, *Chem. Rev.* **2005**, *105*, 3842.
[7] M. K. Cyranski, *Chem. Rev.* **2005**, *105*, 3773.
[8] A. I. Boldyrev, L.-S. Wang, *Chem. Rev.* **2005**, *105*, 3716.
[9] F. Feixas, E. Matito, J. Poater, M. Solà, *WIREs Comput. Mol. Sci.* **2013**, *3*, 105.
[10] I. Casademont-Reig, E. Ramos-Cordoba, M. Torrent-Sucarrat, E. Matito, *Aromaticity: Modern Computational Methods and Applications*, chapter Aromaticity descriptors based on electron delocalization, pages 235–258, Elsevier, The Netherlands **2021**.
[11] M. Giambiagi, M. S. de Giambiagi, K. C. Mundim, *Struct. Chem.* **1990**, *1*, 423.
[12] K. C. Mundim, M. Giambiagi, M. S. de Giambiagi, *J. Phys. Chem.* **1994**, *98*, 6118.
[13] R. Ponec, F. Uhlik, *Croat. Chem. Acta* **1996**, *69*, 941.
[14] M. Giambiagi, M. S. de Giambiagi, C. D. dos Santos Silva, A. P. de Figueiredo, *Phys. Chem. Chem. Phys.* **2000**, *2*, 3381.
[15] P. Bultinck, R. Ponec, S. Van Damme, *J. Phys. Org. Chem.* **2005**, *18*, 706.
[16] J. Cioslowski, E. Matito, M. Solà, *J. Phys. Chem. A* **2007**, *111*, 6521.
[17] F. Feixas, E. Matito, J. Poater, M. Solà, *J. Comput. Chem.* **2008**, *29*, 1543 .

[18] F. Feixas, J. Jiménez-Halla, E. Matito, J. Poater, M. Solà, *J. Chem. Theory Comput.* **2010**, *6*, 1118.
[19] A. Szabo, N. Ostlund, Dover Books on Chemistry **1989**.
[20] R. S. Mulliken, *J. Chem. Phys.* **1955**, *23*, 1833.
[21] A. M. Pendás, M. A. Blanco, E. Francisco, *J. Comput. Chem.* **2007**, *28*, 161.
[22] E. Matito, M. Solà, P. Salvador, M. Duran, *Faraday Discuss.* **2007**, *135*, 325.
[23] Á. M. Pendás, E. Francisco, D. Suárez, A. Costales, N. Díaz, J. Munárriz, T. Rocha-Rinza, J. M. Guevara-Vela, *Phys. Chem. Chem. Phys.* **2023**, *25*, 10231.
[24] R. F. W. Bader, *Atoms in Molecules: A Quantum Theory*, Oxford University Press, Oxford **1990**.
[25] E. Matito, J. Poater, M. Solà, M. Duran, P. Salvador, *J. Phys. Chem. A* **2005**, *109*, 9904.
[26] E. Matito, M. Solà, M. Duran, P. Salvador, *J. Phys. Chem. A* **2006**, *110*, 5108.
[27] R. Ponec, D. L. Cooper, *J. Mol. Struct.* **2005**, *727*, 133.
[28] W. Heyndrickx, P. Salvador, P. Bultinck, M. Solà, E. Matito, *J. Comput. Chem.* **2011**, *32*, 386.
[29] M. Rodríguez-Mayorga, E. Ramos-Cordoba, P. Salvador, M. Solà, E. Matito, *Mol. Phys.* **2016**, *114*, 1345.
[30] F. W. Biegler-Konig, R. F. W. Bader, T.-H. Tang, *J. Comput. Chem.* **1982**, *3*, 317.
[31] E. Matito, *Phys. Chem. Chem. Phys.* **2016**, *18*, 11839.
[32] I. Mayer, *Chem. Phys. Lett.* **1983**, *97*, 270.
[33] T. Kar, A. B. Sannigrahi, *J. Mol. Struct.* **1988**, *165*, 47.
[34] P.-O. Löwdin, *J. Chem. Phys.* **1950**, *18*, 365.
[35] Q. Sun, G. K.-L. Chan, *J. Chem. Theory Comput.* **2014**.
[36] A. E. Reed, R. B. Weinstock, F. Weinhold, *J. Chem. Phys.* **1985**, *83*, 735.
[37] G. Knizia, *J. Chem. Theory Comput.* **2013**.
[38] Q. Sun, T. C. Berkelbach, N. S. Blunt, G. H. Booth, S. Guo, Z. Li, J. Liu, J. D. McClain, E. R. Sayfutyarova, S. Sharma, et al., *WIREs Comput. Mol. Sci.* **2018**, *8*, e1340.
[39] Q. Sun, X. Zhang, S. Banerjee, P. Bao, M. Barbry, N. S. Blunt, N. A. Bogdanov, G. H. Booth, J. Chen, Z.-H. Cui, J. J. Eriksen, Y. Gao, S. Guo, J. Hermann, M. R. Hermes, K. Koh, P. Koval, S. Lehtola, Z. Li, J. Liu, N. Mardirossian, J. D. McClain, M. Motta, B. Mussard, H. Q. Pham, W. P. Artem Pulkin, P. J. Robinson, E. Ronca, E. R. Sayfutyarova, M. Scheurer, H. F. Schurkus, J. E. T. Smith, C. Sun, S.-N. Sun, S. Upadhyay, L. K. Wagner, X. Wang, A. White, J. D. Whitfield, M. J. Williamson, S. Wouters, J. Yang, J. M. Yu, T. Zhu, T. C. Berkelbach, S. Sharma, A. Y. Sokolov, G. K.-L. Chan, *J. Chem. Phys.* **2020**.
[40] M. Kállay, P. R. Nagy, D. Mester, Z. Rolik, G. Samu, J. Csontos, J. Csóka, P. B. Szabó, L. Gyevi-Nagy, B. Hégely, et al., *J. Chem. Phys.* **2020**, *152*.
[41] S. G. Balasubramani, G. P. Chen, S. Coriani, M. Diedenhofen, M. S. Frank, Y. J. Franzke, F. Furche, R. Grotjahn, M. E. Harding, C. Hättig, et al., *J. Chem. Phys.* **2020**, *152*.
[42] H.-J. Werner, P. J. Knowles, F. R. Manby, J. A. Black, K. Doll, A. Heßelmann, D. Kats, A. Köhn, T. Korona, D. A. Kreplin, et al., *J. Chem. Phys.* **2020**, *152*.
[43] M. Mandado, P. Bultinck, M. J. González-Moa, R. A. Mosquera, *Chem. Phys. Lett.* **2006**, *433*, 5.
[44] I. Casademont-Reig, T. Woller, J. Contreras-García, M. Alonso, M. Torrent-Sucarrat, E. Matito, *Phys. Chem. Chem. Phys.* **2018**, *20*, 2787.
[45] E. Matito, M. Duran, M. Solà, *J. Chem. Phys.* **2005**, *122*, 014109.
[46] E. Matito, B. Silvi, M. Duran, M. Solà, *J. Chem. Phys.* **2006**, *125*, 024301.
[47] C. F. Matta, J. Hernandez-Trujillo, *J. Phys. Chem. A* **2003**, *107*, 7496.
[48] J. Poater, X. Fradera, M. Duran, M. Solà, *Chem. Eur. J.* **2003**, *9*, 400.
[49] I. Sumar, R. Cook, P. W. Ayers, C. F. Matta, *Phys. Scr.* **2015**, *91*, 013001.
[50] M. J. Timm, C. F. Matta, L. Massa, L. Huang, *J. Phys. Chem. A* **2014**, *118*, 11304.
[51] A. C. Castro, E. Osorio, J. O. C. Jiménez-Halla, E. Matito, W. Tiznado, G. Merino, *J. Chem. Theory Comput.* **2010**, *6*, 2701.
[52] S. H. Vosko, L. Wilk, M. Nusair, *Can. J. Phys.* **1980**, *58*, 1200.
[53] J. Sancho-García, A. Pérez-Jiménez, *Phys. Chem. Chem. Phys.* **2007**, *9*, 5874.
[54] M. Torrent-Sucarrat, S. Navarro, F. P. Cossío, J. M. Anglada, J. M. Luis, *J. Comput. Chem.* **2017**, *38*, 2819.
[55] I. Casademont-Reig, E. Ramos-Cordoba, M. Torrent-Sucarrat, E. Matito, *Molecules* **2020**, *25*, 711.
[56] I. Casademont-Reig, R. Guerrero-Avilés, E. Ramos-Cordoba, M. Torrent-Sucarrat, E. Matito, *Angew. Chem. Int. Ed.* **2021**, *60*, 24080.
[57] I. Casademont-Reig, L. Soriano-Agueda, E. Ramos-Cordoba, M. Torrent-Sucarrat, E. Matito, *Angew. Chem. Int. Ed.* **2022**, *61*, e202206836.
[58] Q. Sun, T. Berkelbach, N. Blunt, G. Booth, S. Guo, Z. Li, J. Liu, J. McClain, E. Sayfutyarova, S. Sharma, S. Wouters, G.-L. Chan, *Comput. Mol. Sci.* **2018**.
[59] Q. Sun, *J. Comput. Chem.* **2015**.
[60] E. Matito, ESI-3D: Electron Sharing Indices Program for 3D Molecular Space Partitioning **2015**, institute of Computational Chemistry and Catalysis, University of Girona, Catalonia, Spain.
[61] T. A. Keith, AIMAll (Version 14.11.23) **2014**, tK Gristmill Software, Overland Park KS, USA (aim.tkgristmill.com).
[62] M. J. Frisch, G. W. Trucks, H. B. Schlegel, G. E. Scuseria, M. A. Robb, J. R. Cheeseman, G. Scalmani, V. Barone, G. A. Petersson, H. Nakatsuji, X. Li, M. Caricato, A. V. Marenich, J. Bloino, B. G. Janesko, R. Gomperts, B. Mennucci, H. P. Hratchian, J. V. Ortiz, A. F. Izmaylov, J. L. Sonnenberg, D. Williams-Young, F. Ding, F. Lipparini, F. Egidi, J. Goings, B. Peng, A. Petrone, T. Henderson, D. Ranasinghe, V. G. Zakrzewski, J. Gao, N. Rega, G. Zheng, W. Liang, M. Hada, M. Ehara, K. Toyota, R. Fukuda, J. Hasegawa, M. Ishida, T. Nakajima, Y. Honda, O. Kitao, H. Nakai, T. Vreven, K. Throssell, J. A. Montgomery, Jr., J. E. Peralta, F. Ogliaro, M. J. Bearpark, J. J. Heyd, E. N. Brothers, K. N. Kudin, V. N. Staroverov, T. A. Keith, R. Kobayashi, J. Normand, K. Raghavachari, A. P. Rendell, J. C. Burant, S. S. Iyengar, J. Tomasi, M. Cossi, J. M. Millam, M. Klene, C. Adamo, R. Cammi, J. W. Ochterski, R. L. Martin, K. Morokuma, O. Farkas, J. B. Foresman, D. J. Fox, Gaussian~16 Revision C.01 **2016**, gaussian Inc. Wallingford CT.
[63] J. G. Ángyán, M. Loos, I. Mayer, *J. Phys. Chem.* **1994**, *98*, 5244.
[64] X. Fradera, M. A. Austen, R. F. W. Bader, *J. Phys. Chem. A* **1999**, *103*, 304.
[65] M. Solà, *Front. Chem.* **2013**, *1*, 66422.
[66] G. Portella, J. Poater, M. Sola, *J. Phys. Org. Chem.* **2005**, *18*, 785.
[67] R. L. Fulton, *J. Phys. Chem.* **1993**, *97*, 7516.
[68] C. García-Fernández, E. Sierda, M. Abadia, B. E. C. Bugenhagen, M. H. Prosenc, R. Wiesendanger, M. Bazarnik, J. E. Ortega, J. Brede, E. Matito, A. Arnau, *J. Phys. Chem. C* **2017**, *121*, 27118.
[69] S. Escayola, J. Labella, D. Szczepanik, A. Poater, T. Torres, M. Solà, E. Matito, *submitted* **2024**.
[70] L.-F. Cui, X. Huang, L.-M. Wang, D. Y. Zubarev, A. I. Boldyrev, J. Li, L.-S. Wang, *J. Am. Chem. Soc.* **2006**, *128*, 8390.
[71] L.-F. Cui, X. Huang, L.-M. Wang, J. Li, L.-S. Wang, *J. Phys. Chem. A* **2006**, *110*, 10169.
[72] Z. Chen, S. Neukermans, X. Wang, E. Janssens, Z. Zhou, R. E. Silverans, R. B. King, P. v R Schleyer, P. Lievens, *J. Am. Chem. Soc.* **2006**, *128*, 12829.
[73] L. Zhao, R. Grande-Aztatzi, C. Foroutan-Nejad, J. M. Ugalde, G. Frenking, *ChemistrySelect* **2017**, *2*, 863.
[74] J.-R. Deng, D. Bradley, M. Jirásek, H. L. Anderson, M. D. Peeks, *Angew. Chem. Int. Ed.* **2022**, *134*, e202201231.
[75] I. Casademont-Reig, T. Woller, V. García, J. Contreras-García, W. Tiznado, M. Torrent-Sucarrat, E. Matito, M. Alonso, *Chem. Eur. J.* **2023**, *29*, e202202264.
[76] P. Preethalayam, N. Proos Vedin, S. Radenković, H. Ottosson, *J. Phys. Org. Chem.* **2023**, *36*, e4455.
[77] T. Janda, C. Foroutan-Nejad, *Comput. Phys. Commun.* **2018**, *19*, 2357.
[78] Z. Badri, C. Foroutan-Nejad, *Phys. Chem. Chem. Phys.* **2016**, *18*, 11693.
[79] C. Foroutan-Nejad, *J. Org. Chem.* **2023**, *88*, 14831.
[80] M. Orozco-Ic, J. Barroso, R. Islas, G. Merino, *ChemistryOpen* **2020**, *9*, 657.
[81] M. Orozco-Ic, L. Soriano-Agueda, D. Sundholm, E. Matito, G. Merino, *Chem. Sci.* 10.1039/d4sc02269f .
[82] E. Matito, P. Salvador, J. Styszyński, *Phys. Chem. Chem. Phys.* **2013**, *15*, 20080.
[83] E. Steiner, P. W. Fowler, *J. Phys. Chem. A* **2001**, *105*, 9553.
[84] S. Fias, P. W. Fowler, J. L. Delgado, U. Hahn, P. Bultinck, *Chem. Eur. J.* **2008**, *14*, 3093.

Manuscript received: March 31, 2024
Accepted manuscript online: May 21, 2024
Version of record online: July 22, 2024